

Working Surface Science Model for the Phillips Ethylene Polymerization Catalyst: Preparation and Testing

P. C. Thüne,[†] C. P. J. Verhagen,[†] M. J. G. van den Boer,[‡] and J. W. Niemantsverdriet^{*,†}

*Schuit Institute of Catalysis, Eindhoven University of Technology, 5600 MB Eindhoven, The Netherlands, and
DSM Research, Industrial Chemistry and Catalysis, 6160 MD Geleen, The Netherlands*

Received: May 30, 1997[®]

A surface science model for the Phillips ethylene polymerization catalyst has been prepared, by impregnating aqueous CrO₃ on a flat silicium (100) substrate covered by amorphous silica. Impregnating in a spin-coating technique offers control over the chromium loading, which was varied between 0.4 and 4.0 Cr/nm². After impregnation chromium is dispersed molecularly at loadings smaller than 2 Cr/nm². Upon calcination chromium is anchored to the support over Cr–O–Si ester bonds, although a fraction is lost from the surface due to volatilization, as could be established with X-ray photoelectron spectroscopy. The model catalyst polymerizes ethylene at 160 °C and atmospheric pressure after being activated in 80/20 He/O₂ at 650 °C, confirming its validity as a model for the industrial catalyst.

Introduction

Highly dispersed chromium oxide supported on silica or silica/alumina is an industrially important catalyst for ethylene polymerization. The well-known Phillips catalyst^{1,2} consists of less than 1 wt % Cr, impregnated commonly as aqueous CrO₃ on high surface area silica (±300 m²/g), which corresponds to about 0.4 Cr/nm² only. The raw catalyst is activated at at least 550 °C in dry air, yielding anchored Cr[VI]-oxide (along with some inactive Cr₂O₃) on a dehydroxylized support. Upon polymerization with ethylene the chromium is reduced, probably to a Cr[III] state.³ Despite continuous and extensive research for more than 40 years now, there is little understanding of the Phillips catalyst on a molecular level.

The reason for this lies probably in the complex redox and coordination chemistry of chromium in combination with the heterogeneous silica surfaces. As a result the supported chromium may be present on the support in a mixture of different valences and coordination environments, depending on the exact preparation. The nature of the silica support (e.g. specific surface area, porosity, and concentration of surface hydroxyls), the Cr loading, the activation method (e.g. maximum temperature, heating rate, total calcination time, and calcination atmosphere), and further chemical treatments (e.g. reduction with C₂H₄, CO, H₂, or metal alkyls, temperature, etc.) all influence the chemical state of the supported chromium. Furthermore, characterization techniques have their limitations, in particular when applied on catalysts with mixed contents as low as that of the Phillips catalyst. Consequently, results obtained by different groups are difficult to compare, and there is still controversy about the state of the supported chromium species. For example, after calcination the anchored Cr[VI] may be present as mono-, di-, or even polychromate.² McDaniel⁴ (investigating the CrO₃ saturation loading) and Hierl and Kraus⁵ (using a gravimetric method) concluded that CrO₃ binds to the silica support mainly as a monochromate species upon calcination. However, Zecchina et al.⁶ inferred from hydroxyl population measurements that anchored CrO₃ is almost exclusively present as dichromate on silica supports. Applying diffuse reflectance ultraviolet spectroscopy, Weckhuysen et al.⁷ found

mainly dichromate (chromate/dichromate ratio = 0.62) present on calcined silica even at extremely low loadings (0.2 wt % Cr on 735 m²/g silica gel).

Ultrahigh-vacuum spectroscopic techniques are potentially very powerful for the desired microscopic characterization of catalysts in general, as they provide direct information originating from the atoms and molecules on the surface. However, with industrial catalysts the active phase is usually hidden inside a porous, spongelike, high surface area support, e.g. silica, and most of the active phase is hidden inside the pores, out of reach for the surface spectroscopist. Moreover, these supports are nonconductive, and thus the sample will charge when applying electron- or ion-releasing techniques such as X-ray photoelectron spectroscopy (XPS), secondary ion mass spectroscopy (SIMS), or ion scattering. To avoid these complications, model catalysts have been prepared on flat, conducting substrates. (For a review of surface science model catalysts see ref 8.)

Magni and Somarjai recently prepared a surface science model for the TiCl₄/MgCl₂ Ziegler–Natta catalyst in ultrahigh vacuum^{9,10} by gas phase deposition using polycrystalline gold foil as the conducting substrate.

We have now embarked to explore the Cr/SiO₂ system using two model supports and surface science techniques. The first one is prepared on flat Si(100) wafers, which are covered with a thin (~4 nm) layer of amorphous silica. This support is impregnated with aqueous CrO₃ using the spin-coating technique,^{11–13} which gives control over Cr loading and mimics the conventional pore-volume impregnation used in industry for high surface area silica gels. This approach has already successfully been applied to create a working surface science model of the MoS₂ and CoMoS hydrodesulfurization catalyst.^{14–16}

To complement the flat model support, we use silica spheres, often referred to as Stöber spheres, which also yield catalysts with exposed active sites.^{8,17,18} This model allows the use of infrared spectroscopy (DRIFT) to characterize the surface silanols of the support as well as the produced polymer.

While anticipating that our model catalyst approach will eventually contribute to the understanding of the challenging Cr_{ox}/silica system on a molecular level, in this first paper we want to show that our models exhibit essential features of their “real” counterparts, such as anchoring of a Cr-oxo species to

[†] Eindhoven University of Technology.

[‡] DSM Research.

[®] Abstract published in *Advance ACS Abstracts*, September 1, 1997.

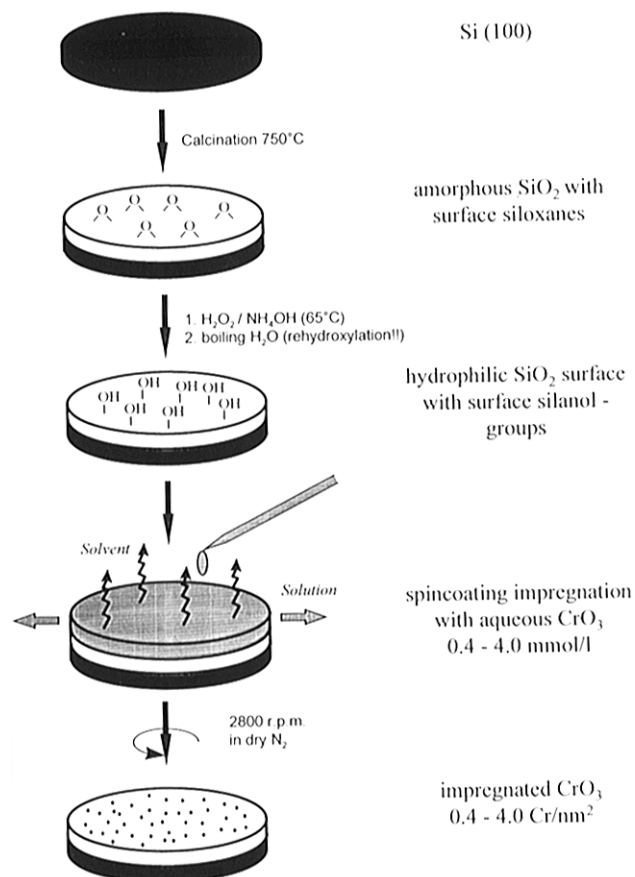


Figure 1. Preparation scheme of the $\text{Cr}_{\text{ox}}/\text{SiO}_2/\text{Si}(100)$ model catalysts.

the silica support upon calcination and, most essentially, catalytic activity for the ethylene polymerization.

Experimental Section

Preparation of the $\text{Cr}_{\text{ox}}/\text{SiO}_2/\text{Si}(100)$ Model. Silicon wafers with (100) surface orientation were calcined in air at 750 °C to form an amorphous SiO_2 overlayer. The calcined wafers were then cleaned in a mixture of H_2O_2 and NH_4OH (3/2 v/v) at 65 °C, rehydroxylized in boiling water, and finally covered with an aqueous CrO_3 solution (0.4–4.0 mmol/L). The hydroxyl population of the rehydroxylized surface could not be quantified yet. Next the sample was placed in a homemade spin-coat apparatus under dry nitrogen. Spin-coating the $\text{SiO}_2/\text{Si}(100)$ wafers at 2800 rpm yielded catalyst-precursor loadings between 0.4 and 4.0 Cr/nm^2 .¹³ The procedure is illustrated in Figure 1.

The precursor was calcined in helium/oxygen (80/20) (He 99.999%, O_2 99.995% (Hoekloos), purified with molecular sieve 4 Å (Ueticon) at a heating rate of 10 K/s up to a maximum temperature of 450–650 °C, which is held for 15 min. To remove all traces of water prior to calcination, the whole reactor was dried at 150 °C under vacuum until the pressure at the turbomolecular pump stabilized at 2×10^{-5} mbar. Polymerization tests were done with ethylene (99.95% (Hoekloos), purified with BASF catalyst R 3-11 (Chrompack) and molecular sieves 4 Å), at 160 °C and atmospheric pressure. This relatively high polymerization temperature was chosen in order to reduce the induction period prior to polymerization.

Stöber silica spheres were prepared according to refs 18 and 19. A mixture of 433.4 mL of ethanol (Merck p.a.), 15.66 mL of water, 18.96 mL of NH_4OH (Merck, 25%, p.a.), and 31.90 mL of tetraethyl orthosilicate (TEOS) (Across, 98%) was stirred at room temperature for 24 h. The liquid phase was then evaporated in vacuum at 40 °C, and the silica spheres were

further dried at 110 °C in air. The thus prepared spheres had a BET surface area of 25.4 m^2/g . They were impregnated with chromium(III) nitrate nonahydrate ($\text{Cr}(\text{NO}_3)_3 \cdot 9\text{H}_2\text{O}$ 99.99+%, Aldrich) to reach a loading of 0.4 Cr/nm^2 using the following precipitation technique. A suspension of the unloaded silica spheres in aqueous $\text{Cr}(\text{NO}_3)_3$ was made slightly acidic ($\text{pH} = 4.0$) with nitric acid. Then 0.01 M NH_4OH was slowly injected via a capillary under vigorous stirring until the pH of the suspension had reached a value of 7.5 (~5 h), at which point the chromium has precipitated quantitatively onto the silica spheres as $\text{Cr}(\text{OH})_3$ ($k_{\text{sp}} \approx 10^{-30}$). Afterwards the liquid phase was evaporated in vacuum at 40 °C and the silica spheres were dried at 110 °C in air. The impregnated spheres were further treated in the same way as the flat model. The silica spheres change color during the chemical treatment as expected: blue-green after impregnation ($\text{Cr}(\text{OH})_3$), yellow-orange after calcination at 650 °C (surface mono-/dichromate), pale green-gray upon contact with ethylene at 160 °C.

XPS Sample Pretreatment and Spectra Processing. The Cr/SiO_2 spheres were calcined and treated with ethylene in a quartz tube reactor and transferred to the UHV apparatus via a mBraun glovebox (MP 150–GII), where they were pressed on indium foil and mounted in a sealed transfer chamber connectable to the XPS apparatus. As the calcined $\text{Cr}_{\text{ox}}/\text{SiO}_2/\text{Si}(100)$ model proved to be extremely sensitive to impurities and water even at concentrations as low as 1 ppm that are usually present inside the glovebox, calcination studies were performed inside a homemade reaction chamber directly connected to the XPS. Before transfer to the XPS chamber the reaction chamber is evacuated to 2×10^{-5} mbar.

XPS measurements are done in a VG-Escalab 200 spectrometer using an aluminum anode ($\text{Al K}\alpha = 1486.3$ eV) operating at 510 W with a background pressure of 2×10^{-9} mbar. Spectra are recorded using the VGS 5000 data system within 2 h, to obtain a good signal to noise ratio. However, since $\text{Cr}[\text{VI}]$ -oxide is known to decompose rapidly when exposed to X-rays, some spectra were limited to 10 min to obtain the $\text{Cr}[\text{VI}]$ binding energy. All binding energies are referred to the Si 2p at 103.3 eV (SiO_2) to correct for charging (~5 eV on Stöber particles, <1 eV on the flat system). Intensities are normalized to the total Si 2p area ($I_{\text{Si}(\text{total})}$) according to

$$I_{\text{Si}(\text{total})} = I_{\text{SiO}_2} + \frac{\lambda_{\text{SiO}_2} n_{\text{SiO}_2}}{\lambda_{\text{Si}} n_{\text{Si}}} I_{\text{Si}}$$

Here λ is the mean inelastic free path of the Si 2p emission ($\lambda_{\text{SiO}_2} = 3.92$ nm, $\lambda_{\text{Si}} = 3.09$ nm²⁰), n is the atomic density ($n_{\text{SiO}_2} = 3.63 \times 10^{-2}$ mol/cm³, $n_{\text{Si}} = 8.29 \times 10^{-2}$ mol/cm³), and I is the integrated area of the Si 2p peak.

Results and Discussion

Control over Chromium Loading during Spin-Coating Impregnation. First we describe the preparation of the flat model system made by impregnating Cr on a thin SiO_2 layer on a silicon wafer. According to a model proposed by van Hardeveld et al.,¹³ the amount of deposited solute during spin-coating can be predicted quantitatively, with high accuracy. Evaporation of the solvent and radial liquid flow (due to centrifugal forces) of the solution determine the amount of solute, which precipitates on the wafer. Solving the resulting differential equation for a spin-coating experiment with an angular velocity $\omega = 293.2$ s⁻¹ (2800 rpm) at room temperature yields

$$L_{\text{Cr}} = 2.76(t_{\text{evap}})^{-0.5} C_0$$

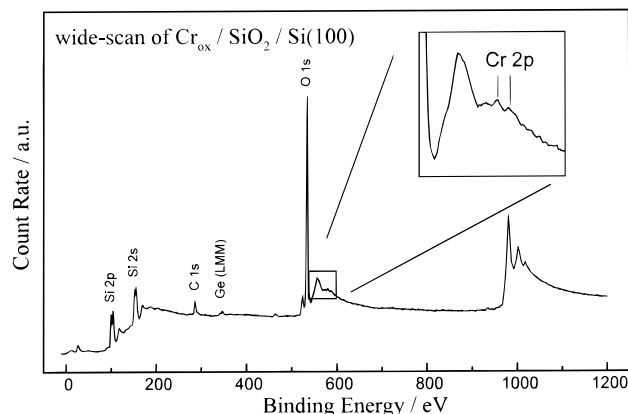


Figure 2. Survey XPS spectrum of a $\text{Cr}_{\text{ox}}/\text{SiO}_2/\text{Si}(100)$ model catalyst after spin-coating impregnation. Loading is $1 \text{ Cr}/\text{nm}^2$. The inset shows an enlargement of the O 1s energy loss region of the spectrum where the Cr 2p emission is observed.

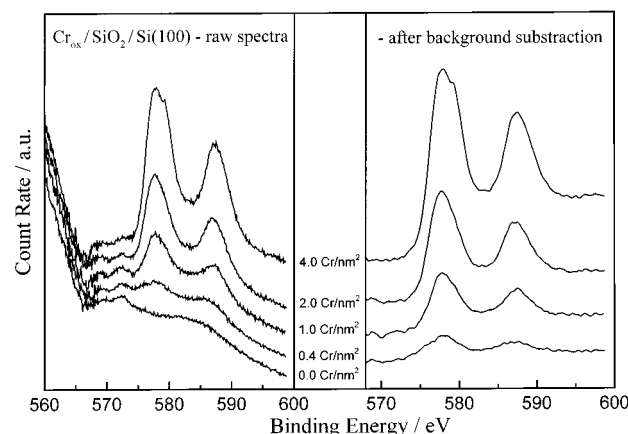


Figure 3. Cr 2p XPS spectra of $\text{Cr}_{\text{ox}}/\text{SiO}_2/\text{Si}(100)$ model catalyst after spin-coating impregnation as a function of Cr loading. Spectra on the left side are as acquired (within 2 h), while on the right side the blanco ($0.0 \text{ Cr}/\text{nm}^2$) has been subtracted.

where L_{Cr} is the loading of the wafer in Cr atoms/ nm^2 , t_{evap} is the evaporation time in seconds, and C_0 is the concentration of the spin-coating solution in mmol/L. If the chromium is dispersed molecularly, we expect a linear relationship between the normalized intensity of the Cr 2p emission $I_{\text{Cr } 2p}/I_{\text{Si } 2p(\text{total})}$ and the chromium loading I_{Cr} as long as the loading is smaller than 1 monolayer ($6.4 \text{ Cr}/\text{nm}^2$ for CrO_3).

To determine the Cr 2p intensity correctly, the nonlinear background under the Cr 2p signal has to be taken into account, as shown in Figure 2 for $\text{Cr}_{\text{ox}}/\text{SiO}_2/\text{Si}(100)$ with a loading of $1 \text{ Cr}/\text{nm}^2$. The weak Cr 2p signal appears superimposed on the energy loss tail of the O 1s emission. We removed this background by subtracting a blanco reference pretreated the same way as the corresponding chromium-loaded samples. This is demonstrated in Figure 3.

Figure 3 (left side) shows the Cr 2p emission of a series of freshly impregnated $\text{Cr}_{\text{ox}}/\text{SiO}_2/\text{Si}(100)$ wafers with loadings between 0.4 and $4.0 \text{ Cr}/\text{nm}^2$ (impregnated with aqueous CrO_3 solution) along with a blanco reference. Subtraction of the blanco (Figure 3, right side) yields the "pure" Cr 2p emission without the curved background due to the O 1s energy loss electrons. The intensities (using a Shirley background) are plotted against the chromium loading in Figure 4. The linear correlation between XPS intensity and loading is indeed observed up to a loading of $2.0 \text{ Cr}/\text{nm}^2$. The intensity at $4.0 \text{ Cr}/\text{nm}^2$ is, however, significantly too small to fit in this linear correlation.

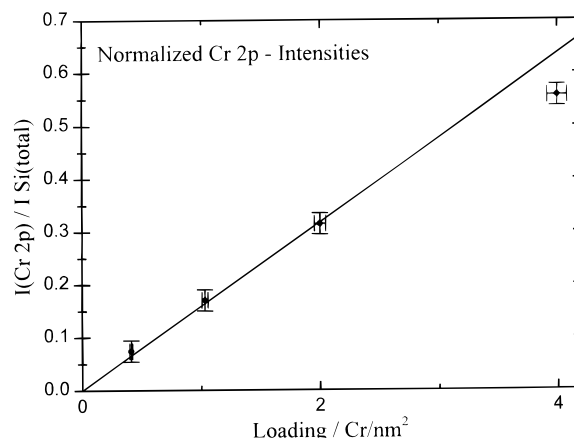


Figure 4. Integrated Cr 2p intensities of $\text{Cr}_{\text{ox}}/\text{SiO}_2/\text{Si}(100)$ model catalysts after spin-coating impregnation as a function of Cr loading.

This finding can tentatively be explained as follows: After wet impregnation the impregnated Cr_{ox} species are coadsorbed on the silica surface together with ~ 1 monolayer of water. As the isoelectric point of silica is rather low (~ 2), this thin water film is acidic and the impregnated chromium is essentially a mixture of mono- and dichromate at relatively low loadings. With increasing loadings tri- and tetrachromate species become important. This picture of hydrated chromium on silica has been proposed by Weckhuysen et al.²¹ The authors found tri- and tetrachromates between 4 and 8 wt % Cr on a $735 \text{ m}^2/\text{g}$ silica, which corresponds to a loading of $\sim 1 \text{ Cr}/\text{nm}^2$. Thus it is reasonable to expect some clustering at loadings of $4 \text{ Cr}/\text{nm}^2$, resulting in a decreased dispersion of the impregnated chromium and therefore in a slightly reduced visibility in XPS.

Anchoring of Chromium to the Support. It is generally accepted that upon calcination in dry air or oxygen chromium-[VI] is anchored to the silica substrate in the form of chromate esters, regardless of which precursor has been used for impregnation. However, the calcination of the Phillips catalyst is a complicated process, that, depending on loading and calcination temperature, may yield mixtures of molecular surface monochromate and dichromate species sometimes along with bulk (inactive) Cr(III)oxide.^{2,7} Although we cannot contribute to the elucidation of the molecular structure of anchored Cr on silica yet, we can prove that our flat $\text{SiO}_2/\text{Si}(100)$ model system is indeed capable of anchoring chromium to the surface and that this process can be followed by XPS.

The X-ray photoelectron spectra in Figure 5 show the Cr 2p emission of $\text{Cr}_{\text{ox}}/\text{SiO}_2/\text{Si}(100)$ models and of two Cr(VI) references. After spin-coat impregnation of $1 \text{ CrO}_3/\text{nm}^2$ the Cr 2p maximum appears at 580.0 eV , the same binding energy that we measured for bulk CrO_3 (Figure 5). Upon calcination at 450°C the binding energy increases to 581.3 eV . This binding energy is in excellent agreement with the 581.6 eV (with Si 2p = 103.5 eV) measured by Merryfield et al.³ for a 1.1 wt % Cr/SiO₂ ($0.42 \text{ Cr}/\text{nm}^2$) catalyst calcined in dry air at 650°C . Moreover we measured a siloxane ester of chromic acid $[\text{CrO}_2(\text{OSi}(\text{C}_6\text{H}_5)_2\text{OSi}(\text{C}_6\text{H}_5)_2\text{O})_2]$; see Figure 5)²² as a reference for surface chromium(VI) esters, which turned out to have the same Cr $2p_{3/2}$ binding energy (Figure 5) as the anchored chromium(VI) on silica. Thus we conclude that the shift in Cr $2p_{3/2}$ binding energy proves the anchoring of Cr to our $\text{SiO}_2/\text{Si}(100)$ model support upon calcination.

Although all of the detectable chromium on the calcined wafer is anchored to the support by ester bonds, it is interesting to note that the intensity of the Cr 2p emission has decreased by about 20%. Such a decrease of intensity upon calcination was only observed on the flat $\text{Cr}_{\text{ox}}/\text{SiO}_2/\text{Si}[110]$ system and not on

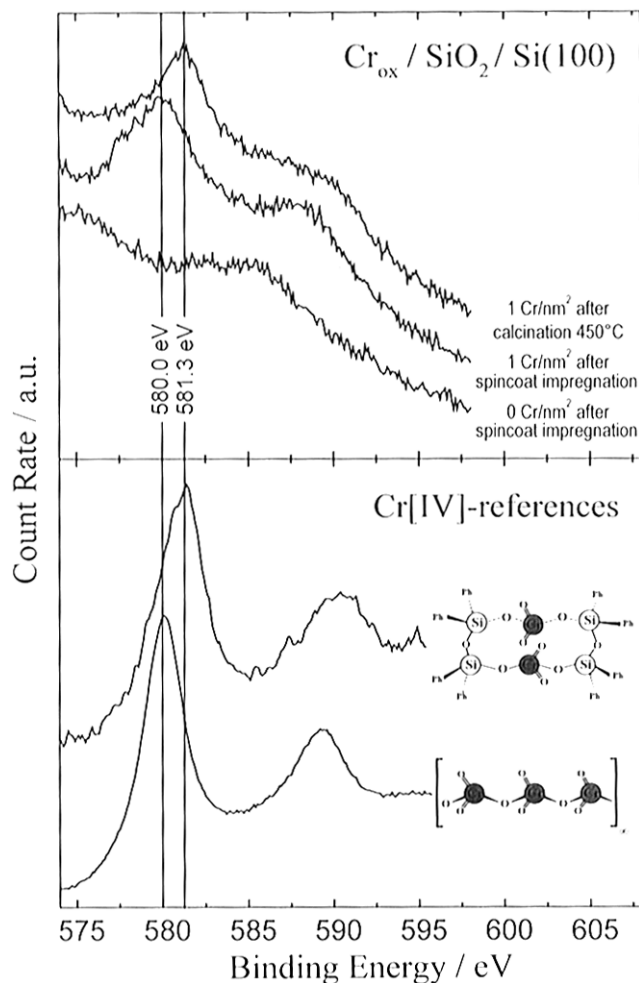


Figure 5. Shift in binding energy of the Cr $2p_{3/2}$ peak of a $\text{CrO}_x/\text{SiO}_2/\text{Si}(100)$ model catalyst (spectra acquired within 10 min) upon calcination in He/O_2 at 450°C (top) and of CrO_3 upon esterification to a siloxanediol (bottom).

the calcined Cr/silica spheres. We believe that some of the impregnated chromium on the flat support was lost due to evaporation.²³ To check this, $\text{SiO}_2/\text{Si}(100)$ wafers impregnated with more than one monolayer of CrO_3 were covered with an unloaded Si wafer and calcined in oxygen at temperatures between 400 and 875°C . After calcination, chromium was detected on the initially clean silica wafer. Although preliminary, these results indicate that impregnated chromium can redistribute on the silica support (inside the pores) via the gas phase upon calcination.²⁴

Polymerization of Ethylene. To polymerize ethylene on the flat $\text{CrO}_x/\text{SiO}_2/\text{Si}(100)$ model catalyst, we need to consider that the latter exposes an active surface of about 1 cm^2 only, which makes the model extremely sensitive to irreversible deactivation by impurities. Thus we chose to protect the surface by embedding the $\text{CrO}_x/\text{SiO}_2/\text{Si}(100)$ wafer in a batch of Cr-impregnated silica spheres. In this experiment the $\text{CrO}_x/\text{SiO}_2/\text{Si}(100)$ wafer was placed in the quartz tube reactor with the active surface facing downward to prevent the silica spheres, which also produced polyethylene, from coming into contact with the active surface of the $\text{CrO}_x/\text{SiO}_2/\text{Si}(100)$ catalyst. Figure 6 shows XPS spectra of a $\text{CrO}_x/\text{SiO}_2/\text{Si}(100)$ catalyst with a loading of $1\text{ Cr}/\text{cm}^2$ after polymerization at 160°C following calcination at 650°C , and the same wafer before reaction. The latter shows some impurity carbon only. After polymerization, the C $1s/\text{Si } 2p$ intensity ratio has increased drastically and the maximum of the C $1s$ emission has shifted by 0.5 eV to lower binding energies. In addition the peak width at half-height has

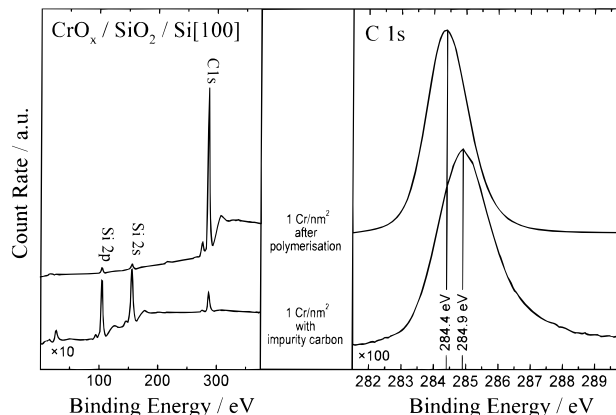


Figure 6. XPS spectra of $\text{CrO}_x/\text{SiO}_2/\text{Si}(100)$ model catalysts with $1\text{ Cr}/\text{nm}^2$. Bottom spectra are after spin-coating impregnation and top spectra after polymerization in ethylene at 160°C and atmospheric pressure following calcination at 650°C .

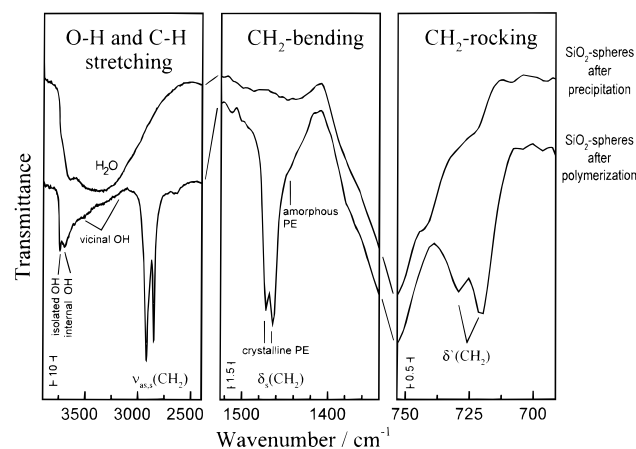


Figure 7. DRIFT spectra of $\text{CrO}_x/\text{SiO}_2$ spheres with $0.4\text{ Cr}/\text{nm}^2$. Top spectra are after precipitation, bottom spectra after calcination at 650°C and polymerization with ethylene at 160°C and atmospheric pressure.

decreased from 1.96 to 1.54 eV and the peak has become more symmetrical. These findings indicate that only one carbon species is observed after polymerization in ethylene, the CH_2 -carbon from polyethylene. The same trends in the C $1s$ emission are observed when comparing Cr/SiO_2 spheres after impregnation and after polymerization (not shown). The formation of polyethylene on the Cr/SiO_2 spheres is confirmed by DRIFT, which shows the development of the CH_2 stretching bands ($\nu_{\text{s,as}}(\text{CH}_2)$, Figure 7, left), the symmetric CH_2 bending band ($\delta_{\text{s}}(\text{CH}_2)$, figure 7, middle), and the CH_2 rocking band ($\delta'(\text{CH}_2)$, Figure 7, right) upon polymerization. Note that CH_3 bands such as $\nu_{\text{as}}(\text{CH}_3) = 2975$ and $\delta_{\text{s}}(\text{CH}_3) = 1368\text{ cm}^{-1}$ are not detectable. The CH_2 symmetric bending and rocking bands appear as doublets ($\delta_{\text{s}}(\text{CH}_2) = 1463$ and 1471 cm^{-1} , $\delta'(\text{CH}_2) = 720$ and 792 cm^{-1}), characteristic of crystalline polyethylene, while the broad shoulder at $\sim 1443\text{ cm}^{-1}$ is associated with amorphous polyethylene.²⁵

Conclusions

A surface science model for the Phillips ethylene polymerization catalyst has been prepared by spin-coating impregnation of aqueous CrO_3 on a $\text{SiO}_2/\text{Si}(100)$ support. Characterization with X-ray photoelectron spectroscopy reveals that the impregnated Cr(VI) -oxide is dispersed molecularly up to a loading of $2\text{ Cr}/\text{nm}^2$. Upon calcination chromium binds to the silica surface, forming $\text{Cr}-\text{O}-\text{Si}$ ester bonds; however, some chromium is lost, probably due to evaporation. The model catalyst

polymerizes ethylene at 160 °C and atmospheric pressure after being calcined at 650 °C. From these findings we conclude that the $\text{Cr}_{\text{ox}}/\text{SiO}_2/\text{Si}(100)$ system is a realistic model that may contribute to a better understanding of the industrial Phillips catalyst in forthcoming experiments.

Acknowledgment. The author would like to thank P. Pypers and B. J. Kip from DSM research for valuable discussions and M. L. W. Vorstenbosch and H. C. L. Abbenhuis for a sample of the chromium(VI)–siloxane complex $[\text{CrO}_2(\text{OSi}(\text{C}_6\text{H}_5)_2\text{OSi}(\text{C}_6\text{H}_5)_2\text{O})]_2$. This work has been supported by the Netherlands Foundation for Chemical Research (SON) with financial aid from the Netherlands Technology Society (STW).

References and Notes

- (1) McDaniel, M. P. *Adv. Catal.* **1985**, 33, 47.
- (2) Weckhuysen, B. M.; Wachs, I. E.; Schoonheydt, R. A. *Chem. Rev.* **1996**, 96, 3327.
- (3) Merryfield, R.; McDaniel, M. P.; Parks, G. *J. Catal.* **1982**, 77, 348.
- (4) McDaniel, M. P. *J. Catal.* **1981**, 67, 71.
- (5) Hierl, G.; Kraus, H. L. *Z. Anorg. Chem.* **1975**, 415, 57.
- (6) Zecchina, A.; Garrone, E.; Ghiotti, G.; Morterra, C.; Borello, E. *J. Phys. Chem.* **1975**, 79, 57.
- (7) Weckhuysen, B.; De Ridder, L. M.; Schoonheydt, R. A. *J. Phys. Chem.* **1993**, 97, 4756.
- (8) Gunter, P. L. J.; Niemantsverdriet, J. W.; Ribeiro, F. H.; Somorjai, G. A. *Catal. Rev.* **1997**, 38, 77.
- (9) Magni, E.; Somorjai, G. A. *Appl. Surf. Sci.* **1996**, 89, 187.
- (10) Magni, E.; Somorjai, G. A. *Surf. Sci.* **1996**, 345, 1.
- (11) Kuipers, E. W.; Laszlo, C.; Wieldraaijer, W. *Catal. Lett.* **1993**, 17, 71.
- (12) Kuipers, E. W.; Doornkamp, C.; Wieldraaijer, W.; van den Berg, R. E. *Chem. Mat.* **1995**, 5, 1367.
- (13) van Hardeveld, R. M.; Gunter, P. L. J.; van IJzendoorn, L. J.; Wieldraaijer, W.; Kuipers, E. W.; Niemantsverdriet, J. W. *Appl. Surf. Sci.* **1995**, 84, 339.
- (14) de Jong, A. M.; Borg, H. J.; van IJzendoorn, L. J.; Soudant, V. G. F. M.; de Beer, V. H. J.; van Veen, J. A. R.; Niemantsverdriet, J. W. *J. Phys. Chem.* **1993**, 97, 6477.
- (15) Muijsers, J. C.; Weber, T.; van Hardeveld, R. M.; Zandbergen, H. W.; Niemantsverdriet, J. W. *J. Catal.* **1995**, 157, 698.
- (16) de Jong, A. M.; de Beer, V. H. J.; van Veen, J. A. R.; Niemantsverdriet, J. W. *J. Phys. Chem.* **1996**, 100, 17722.
- (17) Stöber, W.; Fink, A.; Bohn, E. J. *Colloid Interface Sci.* **1968**, 26, 62.
- (18) Huizinga, D. G.; Smith, D. M. *AIChE J.* **1986**, 32, 1.
- (19) Grieske, H. J. *Eur. Ceram. Soc.* **1994**, 14, 189.
- (20) Tanuma, S.; Powel, C. J.; Penn, D. R. *Surf. Interface Anal.* **1993**, 21, 165.
- (21) Weckhuysen, B. M.; Schoonheydt, R. A.; Jehng, J.-M.; Wachs, I. E.; Cho, S. J.; Ryo, R.; Kijlstra, S.; Poels, E. *J. Chem. Soc., Faraday Trans.* **1995**, 91, 3245.
- (22) Abbenhuis, H. C. L.; Vorstenbosch, M. L. W.; van Santen, R. A. *Inorg. Chem.*, in press.
- (23) Meyer, R. J.; Pietsch, E. H. *Gmelins Handbuch der Anorganischen Chemie, Chrom, Teil B*; 8th ed.; Verlag Chemie: Weinheim, 1962; p 6.
- (24) Goedbloed, M. J.; Niemantsverdriet, J. W. Unpublished results.
- (25) Zerbi, G.; Galiano, G.; Fanti, N. D.; Bains, L. *Polymer* **1989**, 30, 2324.